Effects of Wood Meal Particle Size and Polyethylene Glycol 400 Content on Glycol Lignin Production

Takayuki Suzuki,[a,b] Thi Thi Nge,[c] Yusuke Matsumoto,[c] and Tatsuhiko Yamada [a,c,*]

Glycol lignin (GL) produced *via* acidic solvolysis of cedar wood meal with polyethylene glycol (PEG) is a highly functional material. In this study, the effects of wood meal particle size and amount of PEG added on the properties of PEG400-modified GLs (GL400s) were examined. For this purpose, cedar wood meal with four different particle sizes ranging between 0.18 and 2.00 mm and PEG400 at liquid ratios of 5 and 3 with respect to the wood meal were used. Acidic solvolysis at 140 °C successfully decreased the amount of solid residue with increasing GL400 yield and reaction time at both liquid ratios of 5 and 3. Overall, wood meal size remarkably affected the physical properties of GL400s at low PEG400 content (liquid ratio 3). In addition, the glass transition temperature T_g and thermal flow temperature T_f increased with decreasing wood meal size. Consequently, GL400s with varying thermal properties (T_g = 63 to 97 °C, T_f = 109 to 149 °C) were successfully prepared by adjusting the PEG400 liquid ratios and wood meal size. The data will support the development of a stable manufacturing process for the mass production of GL.

INTRODUCTION

Lignin, one of the major components of plant cell walls, is the most abundant and renewable aromatic biopolymer on earth, comprising 20 to 35% of the lignocellulosic biomass (Dence and Lin 1992). Technical lignin is a lignin derivative obtained through the delignification of lignocellulosic biomass (Achyuthan *et al.* 2010). Its structure varies depending on the delignification process used and the type of lignin present in the lignocellulosic biomass (Kopsahelis *et al.* 2007; Matsushita 2015; Covinich and Area 2024). Most technical lignin, such as kraft lignin (KL), is a by-product of the pulp and paper industry. As the reaction of chemical pulp mills is optimized to produce high-quality cellulosic pulp and paper, the resulting by-product, technical lignin, will not always have suitable properties for materials application. Most technical lignin, including KL, exhibit inadequate thermal flow properties for use as plastic resources. Therefore, chemical modification of technical lignin has been studied (Wang *et al.* 2016; Demuner *et al.* 2019; Argyropoulos *et al.* 2023). Osti *et al.* (2024) reported the modifying of KL with poly (propylene glycol) diglycidyl ether and polyethylene glycol (PEG) to develop functional materials. Rodrigues *et al.* (2023) reported fractionated KL-based phenolic resins, while Shorey *et al.* (2024) reported the preparation of cellulose acetate and oleic acid-esterified KL-based films.

bioresources.cnr.ncsu.edu

Organosolv lignin, another type of technical lignin, is obtained from the organosolv pulping process, which employs an organic solvent or an aqueous solution of organic solvent (Rabelo *et al.* 2023). This process is considered promising for total biomass utilization. A pilot scale implementation of the organosolv process, such as the Alcell (Pye *et al.* 1991), Glycell (Van Nieuwenhove *et al.* 2020), and Formico processes (Anttila *et al.* 2010; Kupiainen *et al.* 2012) has been studied to produce organosolv lignin (Tofani *et al.* 2024). Numerous studies have investigated Alcell lignin-based materials (Ai *et al.* 2021; Beaucamp *et al.* 2021).

Recently, glycols such as PEG were applied to produce a kind of high-performance olganosolv lignin called glycol lignin (GL). Yamada *et al.* (2021) developed a method for producing GL from cedar wood meal *via* acid-catalyzed solvolysis using PEG as an organic solvent (Nge *et al.* 2016). A GL production plant with a wood meal level of 50 kg is currently in operation (Nge *et al.* 2018). GL comprises PEG-modified lignin derivatives, where PEG moieties are introduced for their hydroxyl groups on the benzyl (α) carbons of lignin side chains during PEG solvolysis. Thus, GL exhibits a viscous thermal flow after the glass transition state, which is crucial for thermal processing in material production. Applications of GL as a high-performance material include fiber-reinforced plastics (Kobayashi *et al.* 2018), epoxy resins (Ono *et al.* 2019), and nanocomposite films used as electronic substrate materials (Takahashi *et al.* 2017; Suzuki *et al.* 2018, 2019). To achieve the commercialization of GL materials, it is necessary to reduce production costs to meet market demands, even though the application of GL for high-performance materials remains important. The current GL manufacturing process excessively uses PEG. Although PEG can be recycled (Takata *et al.* 2016), minimizing the amount of PEG used is crucial in reducing energy and raw material costs. In addition, a previous study revealed that the particle size of wood meals significantly influences the stable production of GL with consistent physical properties.

In this study, to establish a low-cost and stable manufacturing process for the mass production of GL, the focus was on the amount of PEG added and reduced the ratio of PEG used in the reaction. Cedar wood meal with four different particle sizes was prepared using a rotatory tap sieve shaker. The effects of the amount of PEG added and wood meal particle size on the physical properties of the resulting GLs were then investigated.

EXPERIMENTAL

Materials

The cedar wood meal (<5 mm) used in this study was supplied by Miyanosato Biomass LLP (Hitachiota Ibaraki, Japan). The wood meal was then sieved using an electric rotary tap sieve shaker (S-1; Teraoka Co., Suita, Japan), which used sieves with a diameter of 200 mm and mesh sizes of 5.00, 2.00, 1.00, 0.840, 0.600, 0.425, and 0.180 mm. The sieved wood meal was classified into XS wood meal (0.180 mm < d < 0.400 mm), S wood meal (0.600 mm < d < 0.840 mm), M wood meal (1.00 mm < d < 2.00 mm), and L wood meal (2.00 mm < d < 5.00 mm) based on its particle size. PEG (BLAUNON PEG-400) was purchased from Aoki Oil Industrial Co., Ltd. Concentrated sulfuric acid (98%), sodium hydroxide aqueous solution (8 mol/L), 2-propanol, and acetic acid were purchased from FUJIFILM Wako Pure Chemical Corporation. HPLC-grade *N*,*N*-dimethylformamide (DMF) and LiBr were purchased from Kanto Chemical Co., Inc. (Tokyo, Japan).

Preparation of GL

Figure 1 shows the preparation procedure of GL. Acidified liquid PEG400 was prepared by adding concentrated sulfuric acid (1.5 wt% with respect to the wood meal) to PEG400 and stirring for 30 min to obtain a homogeneous solvolysis reagent. The classified wood meal (1 g, dry weight basis) was loaded in a 60-mL reaction vessel, followed by acidified PEG400 (wood meal to PEG400 ratio: 1:3 and 1:5, w/w%). The reaction vessel was equipped with a mechanical stirrer, and the mixture was stirred at 300 rpm for 30 min. Subsequently, the reaction vessel was placed in an oil bath and preheated to 140 °C to initiate the acid-catalyzed solvolysis reaction, which was conducted for 30 to 240 min with stirring at 300 rpm. After the solvolysis, the reaction vessel was removed from the oil bath and cooled in an ice-water bath. The reaction mixture was then diluted with 30 mL of 0.1 N NaOH aqueous solution and stirred at 300 rpm for 30 min. The alkaline diluted mixture was filtered through a Buchner funnel (50-mm inner diameter with a 5C filter, Advantec Toyo Co., Ltd., Tokyo, Japan) under reduced pressure. The insoluble solid residue was washed with distilled water (5 mL, four times) and dried at 105 °C overnight. The pH of the resulting filtrate was adjusted to 2.0 using 2 N sulfuric acid while stirring it to isolate PEG400-modified lignin derivatives, which precipitated under acidic pH.
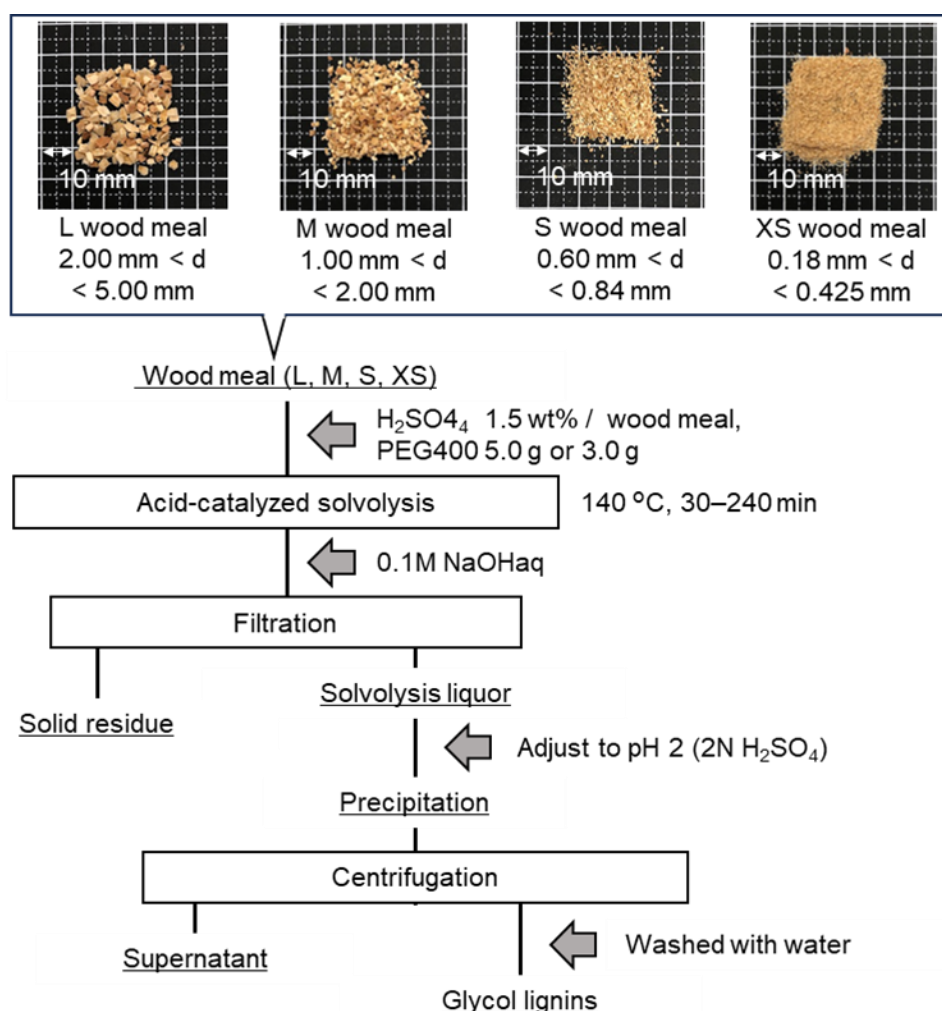
Fig. 1. Procedure for the preparation of glycol lignin (GL400)

The precipitated lignin derivatives, namely GL400, were collected by centrifugation at 3000 rpm for 20 min, followed by successive washing with distilled water (40 mL, three times). The collected GL400 precipitates were vacuum dried for 3 d at room temperature. The yields of the solid residue as well as GL400 were then calculated from the dry weight of the wood meal.

UV Lignin Content

A UV spectrophotometer (V-650, JASCO Corporation, Hachioji, Japan) was used to determine the content of lignin-derived materials in various GL400 samples to evaluate the purity of the samples (Nge *et al.* 2016). The GL400 sample (15 mg) was loaded in a 25-mL measuring flask and dissolved in 2-propanol:0.2 M NaOH (v/v =1:1) (solution A). Solution A (5 mL) was then transferred to a 10-mL measuring flask and diluted with 2-propanol:0.2 M NaOH (v/v = 1:1) (solution B). Solution B (2 mL) was transferred to a 25-mL measuring flask and diluted with 2-propanol:distilled water (v/v = 1:1) (Solution C), where approximately 120 uL of acetic acid was added to adjust pH 5.0 of solution C. The absorbance spectra of the solution were then recorded at 280 nm, and the UV lignin content was calculated using the absorbance coefficient of 23.945 g L^{-1} cm^{-1}, which was a reported value based on Klason lignin content of GL400M (Nge *et al.* 2018).

Fourier Transform Infrared Spectroscopy (FTIR)

Fourier transform-infrared (FTIR) spectroscopy was performed using a spectrometer (Spectrum100; PerkinElmer, Inc., Waltham, Ma, USA) equipped with an attenuated total reflectance (ATR) unit and a single-crystal diamond top plate. The spectra were collected in the range of 4000 to 400 cm^{-1} using 32 scans and a resolution of 4 cm^{-1} and were normalized using the aromatic skeletal vibration band intensity at 1512 cm^{-1} (aromatic ring C=C–C stretching) as an internal standard. The ATR corrections and baseline adjustments were performed before normalization.

Gel Permeation Chromatography (GPC)

The number-average molecular weight (M_n) and weight-average molecular weight (M_w) of the GL400 samples were determined using a GPC apparatus (HLC-8320GPC, Tosoh Co., Tokyo, Japan) equipped with Shodex KD-G, KD-802, and KD-804 (Resonac Corporation) and a UV detector (280 nm). GPC was performed at a column oven temperature of 40 °C, using 10 mM LiBr DMF as the eluent, at a flow rate of 0.7 mL/min. The molecular weight was calibrated using purchased standard samples (M_w: 238, 330, 601, 1050, 1540, 2130, 3170, 4240, 6200, 11100, 17900, 23600, 40100, 41300, 98100, 220000, 504000, 1200000) of Fluka PEG/poly(ethylene oxide) standard ReadyCal sets (Sigma-Aldrich Japan G. K., Tokyo, Japan). GL400 samples were dissolved in the eluent to prepare a 1 mg/mL solution. Before injection, the solution was filtered through a 0.45-μm PTFE syringe filter (Advantec Toyo Co., Ltd., Tokyo, Japan). The M_n, M_w, and polydispersity index (PDI) were calculated using an analysis software (EcoSEC Data Analysis; Tosoh Co., Tokyo, Japan).

Thermomechanical Analysis (TMA)

The glass transition temperature (T_g) and thermal flow temperature (T_f) of the GL400 samples were measured under a nitrogen environment (100 mL/min) using a thermomechanical analyzer (Q400 TMA; TA Instruments-Waters LLC, New Castle, DE, USA). Vacuum-dried and finely ground GL400 samples (8 mg) were loaded into a TGA

platinum sample pan (φ 6 × 2.5 mm), and a flat aluminum plate (φ 4 mm) was placed on top of the sample. A load of 0.05 N was applied, and the sample was heated from room temperature to 200 °C at a heating rate of 5 °C/min. The T_g and T_f were calculated using the TA Universal Analysis Software (Nge *et al.* 2016).

RESULTS AND DISCUSSION

Yields of Fractional Components

The GL400 samples obtained by the acid-catalyzed solvolysis of the four types of wood meal samples (L, M, S, and XS) at PEG400 ratios of 5 and 3 were denoted as 5L-GL400, 5M-GL400, 5S-GL400, and 5XS-GL400, and as 3L-GL400, 3M-GL400, 3S-GL400, and 3XS-GL400, respectively. Figure 2 shows the changes in the amount of solid residue and GL400 yield as a function of reaction time. The GL400 yield increased with decreasing solid residue for all wood meal sizes. Because of the nature of the solid–liquid reaction mixture, the reaction process is expected to be faster for finer grain wood meal sizes than for larger grain sizes in term of accessible surface area. Therefore, at the liquid ratio of 5, the amount of solid residue decreased linearly over the 60-min solvolysis reaction time for all four wood meal samples in the following order: XS > S > M > L (Fig. 2a). The solvolysis reaction rate also gradually decreased until the end of the 240-min reaction. After the 240-min reaction, 42.1%, 43.0%, 40.4%, and 46% solid residues were obtained for the wood meal sizes of XS, S, M, and L, respectively.

A similar linear increasing trend was observed for GL400 yield with an increase in reaction time (0 to 60 min), regardless of the wood meal sizes. It was assumed that the higher reactivity with finer grain size may increase the amount of acid-soluble GL400s. The yield increased slightly as the reaction time progressed from 60 to 240 min (Fig. 2a). Overall, the effect of wood meal size on GL400 yield at the liquid ratio of 5 was negligible at all designated reaction times, where yields of 10 to 11%, 19 to 20%, 23 to 27%, 26 to 28%, and 30 to 34% were produced at 30, 60, 90, 120, and 240 min during the reaction.
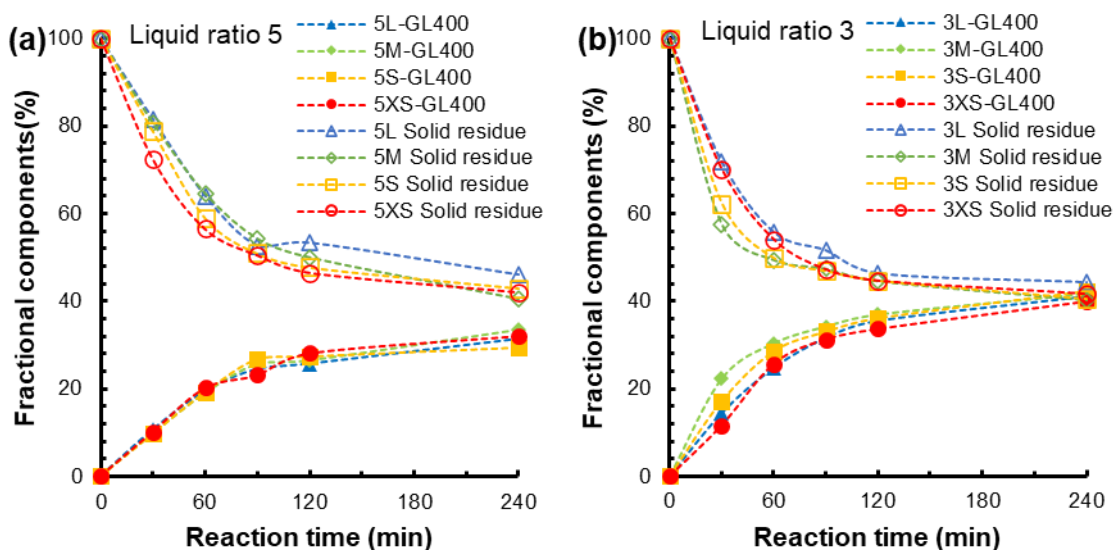
Fig. 2. Yields of GL400s and solid residues as a function of reaction time at liquid ratios of (a) 5 and (b) 3

At the liquid ratio of 3, the amount of solid residue decreased sharply within the 60-min reaction time for all wood meal sizes in the following order: M ≥ S > XS > L (Fig. 2b). These results were different from those observed at the liquid ratio of 5. This suggests that the liquid ratio had a more pronounced effect on the solid residue yield than wood meal size. In addition, the amount of solid residue generated for each wood meal size at the liquid ratio of 3 was lower than that generated at the liquid ratio of 5. After that, the solvolysis reaction rate slowed down and gradually decreased within the 240-min reaction time. For wood meal sizes of M, S, XS, and L, the amounts of solid residue produced after 240 min of reaction time were 40.3%, 40.5%, 41.6%, and 44.5%, respectively. The amount of solid residue remaining at 240 min was similar for both liquid ratios. However, a rather high reactivity was observed at the liquid ratio of 3 for all wood meal sizes within the first 60 min of the reaction.

As expected, GL400 yield exhibited an increasing trend, which agreed with the decreasing trend of solid residue for all wood meal sizes (Fig. 2b). The GL400 yields of 12 to 22%, 25 to 30%, 31 to 34%, 34 to 37%, and 40 to 42% were produced at the 30-, 60-, 90-, 120-, and 240-min reaction times, respectively. Notably, the lower liquid ratio of 3 had a more significant effect on the reaction rate at the early stages of the reaction, resulting in higher GL400s yields at all reaction times compared to the liquid ratio of 5 (Fig. 2a and b).

Tables 1 and 2 present the UV lignin contents of the GL400 samples at liquid ratios of 5 and 3, respectively. The UV lignin content increased with reaction time in all samples. Samples prepared with liquid ratio 3 exhibited higher lignin contents than those prepared with liquid ratio 5, except for wood meal size L. This result was in agreement with the results for GL400 yields (Fig 2). At the reaction time of 240 min, the effect of wood meal size on UV lignin content was not detected for samples prepared at liquid ratio 5. However, the UV lignin content increased with decreasing wood meal size at liquid ratio 3.

Table 1. UV lignin Content, Number-average Molecular Weight (M_n), Weight-Average Molecular Weight (M_w), Poly Dispersity Index (PDI), and Thermal Properties of Glycol Lignin (GL400) for the Liquid Ratio 5

Wood Meal Particle Size	Reaction Time (min)	UV Lignin Content	M_n	M_w	PDI	T_f (°C)	T_g (°C)
L	30	65.8	2500	12810	5.1	62.7	112.3
L	90	75.7	2440	6260	2.6	70.4	117.8
L	240	84.7	2350	5610	2.4	82.3	121.3
M	30	65.9	2440	12700	5.2	63.2	109.2
M	90	74.8	2700	8120	2.9	68.3	116.8
M	240	83.4	2440	5870	2.4	78.1	120.1
S	30	68.7	2480	18340	7.4	66.5	115.3
S	90	76.4	2430	6440	2.7	67.9	115.8
S	240	83.4	2400	5730	2.4	85.0	123.5
XS	30	68.7	2440	14090	5.8	65.9	113.8
XS	90	73.6	2460	6490	2.6	66.1	117.3
XS	240	84.2	2390	5720	2.4	77.5	118.1

Table 2. UV-lignin Content, Number-average Molecular Weight (M_n), Weight-Average Molecular Weight (M_w), Polydispersity Index (PDI), and Thermal Properties of Glycol Lignin (GL400) for the Liquid Ratio 3

Wood Meal Particle Size	Reaction Time (min)	UV Lignin Content (%)	M_n	M_w	PDI	T_f (°C)	T_g (°C)
L	30	70.7	2440	12680	5.2	74.9	118.1
L	90	76.9	2450	6090	2.5	77.6	123.9
L	240	81.4	2790	7450	2.7	87.8	129.8
M	30	72.5	2420	8210	3.4	73.7	115.2
M	90	76.6	2450	6970	2.8	76.1	125.1
M	240	86.3	2610	7870	3.0	90.3	134.3
S	30	71.4	2450	11080	4.5	68.0	114.8
S	90	78.3	2360	6030	2.6	85.4	127.9
S	240	86.4	2580	7210	2.8	93.5	142.0
XS	30	73.6	2550	11660	4.6	70.0	115.9
XS	90	83.1	2750	6310	2.3	91.0	132.1
XS	240	90.0	3040	7760	2.6	97.4	148.7

Chemical Structure of GL400

Figure 3(a) shows the ATR-FTIR spectra of PEG400 and GL400 samples prepared from four types of wood meal at the liquid ratio of 3. These spectra were obtained at the reaction time of 240 min. The FTIR spectrum of PEG400 shows peaks at 3446, 2865, 1350, 1096, and 946 cm^{-1}, which correspond to O–H stretching vibrations, symmetric C–H stretching vibrations of the methylene group, CH$_2$ wagging, C–O stretching, and CH$_2$ rocking vibrations, respectively. The ATR-FTIR spectra of the GL400 samples exhibited characteristic lignin bands at approximately 3399 cm^{-1} (O–H stretching vibrations), 2911 cm^{-1}, 2875 cm^{-1} (C–H stretching vibrations of the methyl and methylene groups), 1596 and 1510 cm^{-1} (aromatic ring C=C–C stretching), 1456 cm^{-1} (C–H deformation), 1427 cm^{-1} (aromatic ring vibration combined with C–H deformation), 1266 cm^{-1} (G ring breathing with C=O stretching), and 1032 cm^{-1} (aromatic C–H in-plane deformation and C–O deformation) (Nge *et al.* 2020). Notably, two new peaks at 1351 and 947 cm^{-1} were observed in the ATR-FTIR spectra of GL400 samples; these peaks correspond to the CH$_2$ wagging and rocking vibrations of PEG400. In addition, a strong C–O stretching vibration peak at 1096 cm^{-1} was observed in the FTIR spectrum of PEG400. Two strong peaks at 1126 cm^{-1} (aromatic-aliphatic ether, C–O–C stretching) and 1088 cm^{-1} (C–O deformation in secondary alcohol and ether) were observed for GL400. These peaks indicate the incorporation of PEG400 moieties into the lignin macromolecules (Nge *et al.* 2018; Nge *et al.* 2020). As shown in Fig. 3a, the effect of wood meal particle size on the structural changes in GL400 samples was not detected. Meanwhile, the intensity of the carbonyl stretching peak in unconjugated ketones and conjugated acids/esters at 1714 cm^{-1} increased with reaction time (Fig. 3b) for all wood meal sizes. As demonstrated in the authors' previous study, the increasing amount of carbonyl structure with the progression of the acidic treatment is a typical characteristic of the acidic degradation of lignocellulosic biomass (Nge *et al.* 2018). A similar spectral pattern was observed in the ATR-FTIR spectra of GL400 samples prepared at the liquid ratio of 5.
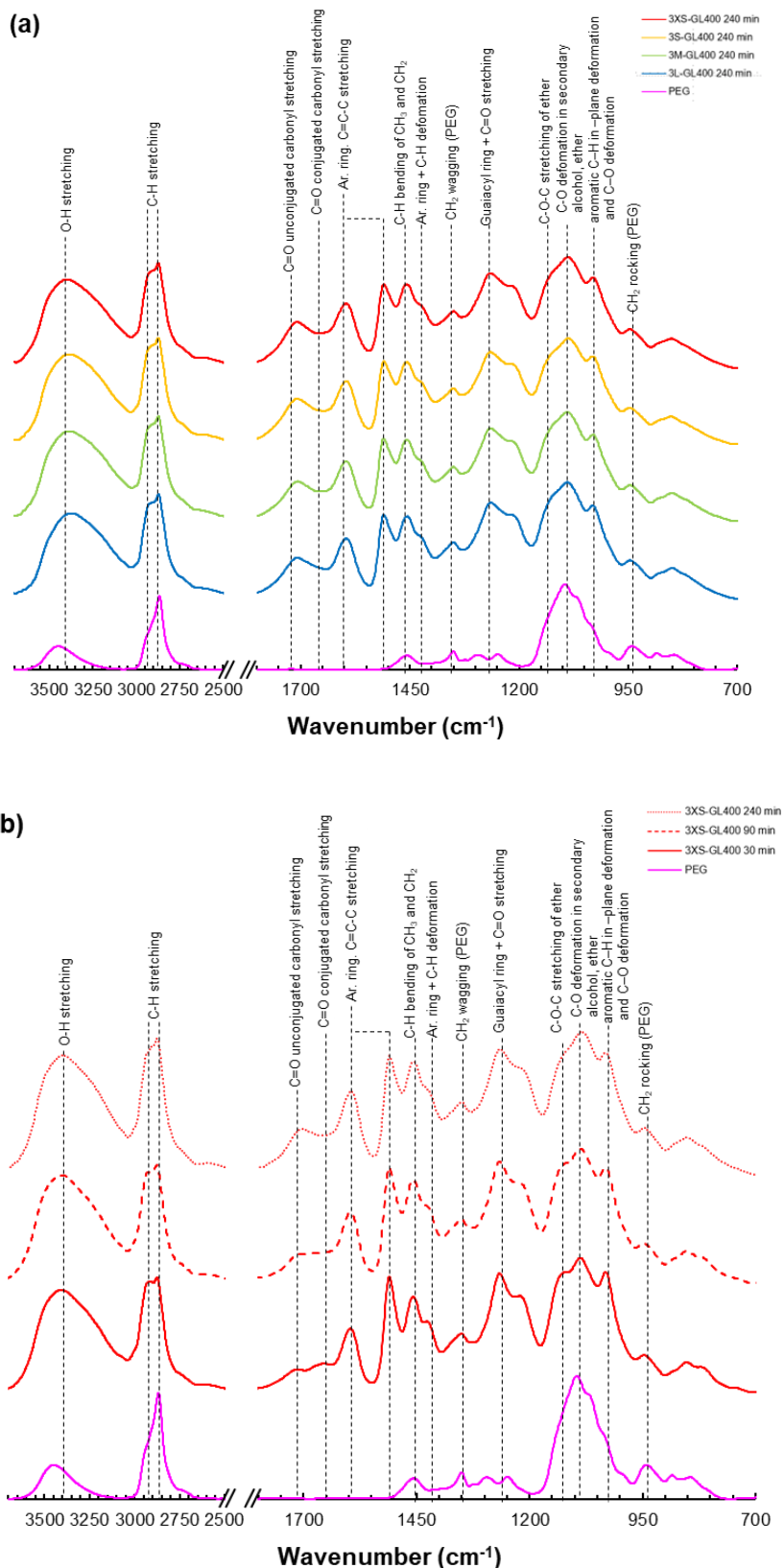
Fig. 3. ATR-FTIR spectra of (a) GL400 samples prepared with liquid ratio 3 (wood meal/PEG400 = 1:3 (w/w)), and four classified wood meal sizes; and (b) 3XS-GL400 sample as a function of reaction time

Molecular Weight Distribution of GL400s

The weight-average (M_w) and number-average (M_n) molecular weights of the GL400 samples prepared at liquid ratios of 5 and 3 are presented in Tables 1 and 2, respectively. The molecular weights of all GL400 samples prepared in this study exhibited bimodal distribution curves (Fig. 4). Similar weight distribution profiles were observed in previous studies (Nge *et al.* 2018). As shown in Fig. 4a (liquid ratio 5), the area under the peak in the high molecular weight distribution region at the 30-min reaction time became significantly reduced and shifted toward the low molecular weight distribution region at the 90-min reaction time. This result indicates the fragmentation of the large GL400 fraction with increasing reaction time. Between the reaction times of 90 to 240 min, the weight distribution curve shifted slightly toward the low molecular weight distribution region for samples containing L-sized wood meal. In contrast, changes in peak height and distribution area were more pronounced in samples with XS-sized wood meal. As described in Table 1 (samples prepared at liquid ratio 5), the average molecular weights (M_w and M_n) decreased with increasing reaction time for all wood meal sizes, except for the M_n value of 5M-GL400-90min. The decrease in M_w values between the reaction times of 30 to 90 min was large, followed by a slight decrease in the value from between 90 to 240 min, where the effect of wood meal size on M_w and M_n was minimal. The M_w and M_n values determined at the 240-min reaction time were in the range of 5600 to 5900 and 2300 to 2400, respectively (Table 1).
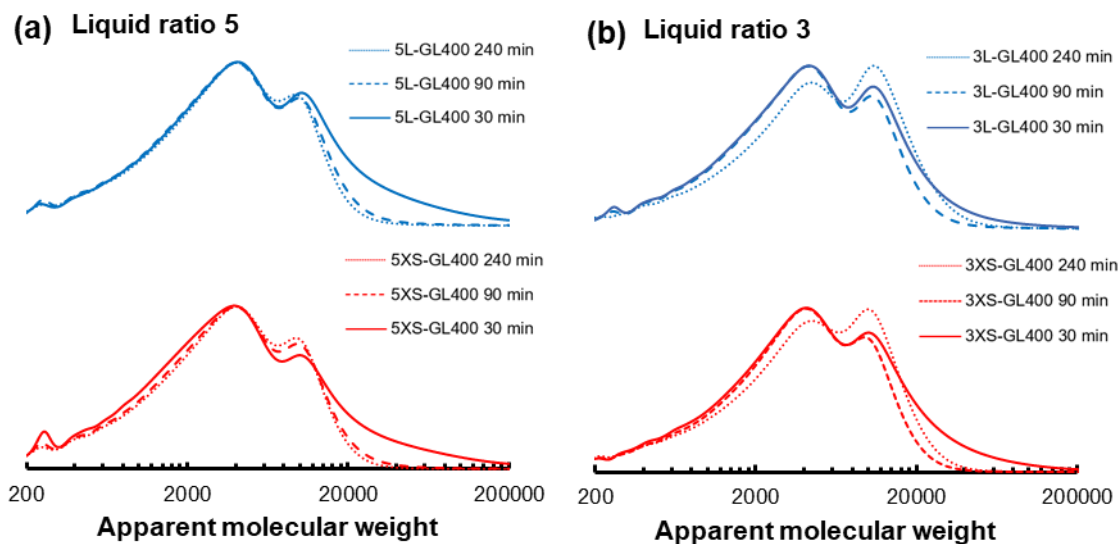
Fig. 4. Size exclusion chromatograms of GL400 samples prepared from wood meal size L and XS as a of function time: (a) liquid ratio 5, (b) liquid ratio 3

Conversely, for samples prepared at the liquid ratio of 3, the bimodal distribution curves (Fig. 4b) changed considerably with increasing reaction time. The area under the peak in the high molecular weight distribution region at the 30-min reaction time was significantly reduced and shifted toward the low molecular weight distribution region at the 90-min reaction time. Subsequently, the peak in the high molecular weight distribution region increased with a simultaneous decrease in the peak in the low molecular weight distribution region. The peak in the low molecular weight distribution region then shifted toward the high molecular weight distribution region for all wood meal sizes (Fig. 4b). The

appearance of the molecular weight distribution curves reflects the M_w and M_n values described in Table 2. At the liquid ratio of 3, the M_w values decreased between the reaction times of 30 to 90 min reaction time and then increased at 240 min. In contrast, M_n values slightly increased with increasing reaction time. This increase in M_n and M_w values was due to acid-induced chemical rearrangements, including condensation and side-chain cleavage reactions, which occurred during the acid-catalyzed solvolysis of wood meal. This reaction was carried out using a reduced amount of PEG400 for a considerably longer time (240 min). Accordingly, increased PDI values were determined for GL400 samples at the 240-min reaction time; however, the effect of wood meal size on PDI values was not detected. The M_w and M_n values determined at the 240-min reaction time were in the range of 7200 to 7900 and 2600 to 3000, respectively (Table 2).

Overall, the effect of liquid ratio, that is, a reduced amount of PEG400, resulted in high M_w and M_n values at the 240-min reaction time for all wood meal sizes. Nevertheless, wood meal size showed little or no effect on the molecular mass of the GL400 samples.

Thermomechanical Analysis of GL400s

Figure 5 shows the TMA curves of GL400 samples prepared at liquid ratios of 5 and 3. The second thermal transition temperature T_f was greater than T_g for all GL400 samples because of the incorporation of PEG400 moieties, as reported in previous studies (Nge *et al.* 2016, 2018). This type of thermal fusion is important for thermal processing during the production of GL-based materials. Both thermal transition temperatures, T_g and T_f, increased with reaction time from 30 to 240 min for both liquid ratios (Fig. 5, Table 1, and Table 2). The effect of wood meal size on the thermal transition temperatures was negligible in samples prepared using the liquid ratio of 5 (Fig. 5a–5c, Table 1). However, at the liquid ratio of 3, both T_g and T_f increased with decreasing wood meal size (Fig. 5e and 5f, Table 2). In addition, T_g due to the molecular motion of rigid lignin side chains represented by derivative peaks composed of two different volume changes at 30- and 90-min reaction time compared to those at 240-min reaction time. This thermal behavior reflects that the fragmentation of lignin macromolecules as well as acid-induced chemical rearrangements, including condensation and side-chain cleavage reactions, occurred as the acid-catalyzed solvolysis reaction progressed. As the reaction time increased, the extent of the reaction in acidic conditions also increased, potentially facilitating chemical rearrangements, including the condensation of lignin fragments, which could increase T_g. Similarly, decreasing wood meal size may affect the extent of the reaction, promoting condensation under acidic conditions, resulting in higher T_g and T_f.

At the liquid ratio of 3, wood meal size considerably influenced the thermal transition temperatures of GL400 samples, where T_g and T_f increased with decreasing wood meal size. In addition, the effect of liquid ratio on the T_g and T_f of GL400 samples was more noticeable at the reduced amount of added PEG400 (liquid ratio 3). The T_g and T_f of liquid ratio 3 samples were higher than those of liquid ratio 5 samples. For example, 3XS-GL400, prepared using XS-sized wood meal, showed a maximum difference of ~20 °C for T_g and ~30 °C for T_f at the 240-min reaction time. In the chemical degradation reaction of solid materials in liquid media, condensation reactions of the degraded products occur more frequently in a smaller amount of liquid media. The GL400 prepared at the lower liquid ratio of 3 showed higher T_g and T_f compared with those prepared at the liquid ratio of 5.

The higher values of T_g and T_f with increasing reaction time as well as decreasing wood meal size agreed with the increase in UV lignin content of the GL400 samples (Tables 1 and 2, Fig. 6). As the UV-lignin content reflects the amount of grafted PEGs, a

higher UV lignin content indicates a lower amount of grafted PEGs, which contributed to the higher T_g and T_f values.
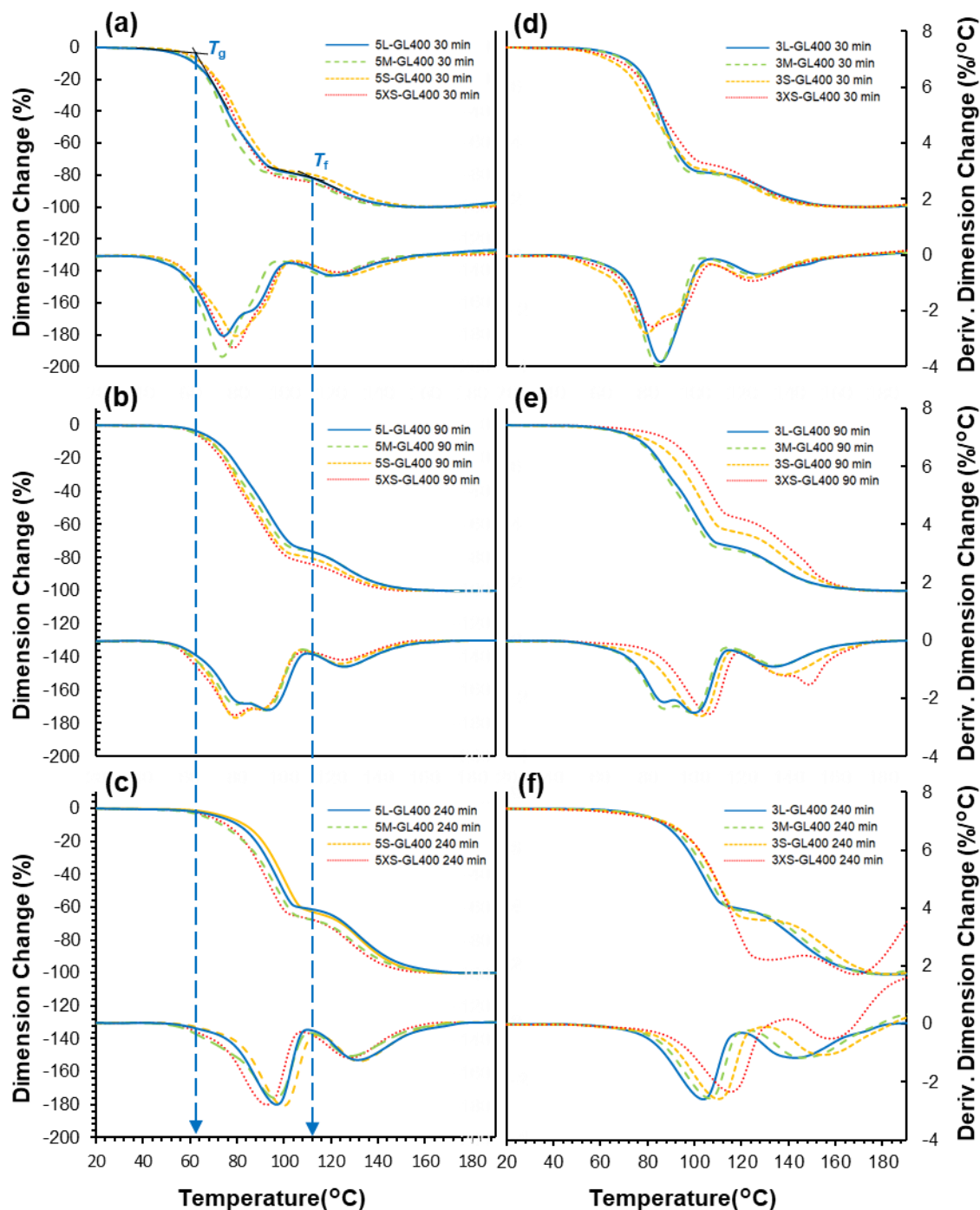
Fig. 5. TMA profiles of GL400s prepared using liquid ratios of 5 (a through c) and 3 (d through f) for (a, d) 30-min, (b, e) 90-min, and (c, f) 240-min reaction time

Figure 6 shows the relationship between UV lignin content and the thermal transition temperatures (T_g and T_f) for both liquid ratios. A noticeable positive correlation was observed at liquid ratio 3, where R^2 values of 0.936 and 0.907 were determined for T_g

and T_f, respectively (Fig. 6b). In contrast, liquid ratio 5 in R^2 values of 0.800 and 0.858 were determined for T_g and T_f, respectively, at liquid ratio 5. Thus, GL400 samples with varying thermal properties (T_g = 63 to 97 °C, T_f = 109 to 149 °C) can be successfully prepared by adjusting the PEG400 liquid ratio and wood meal size.
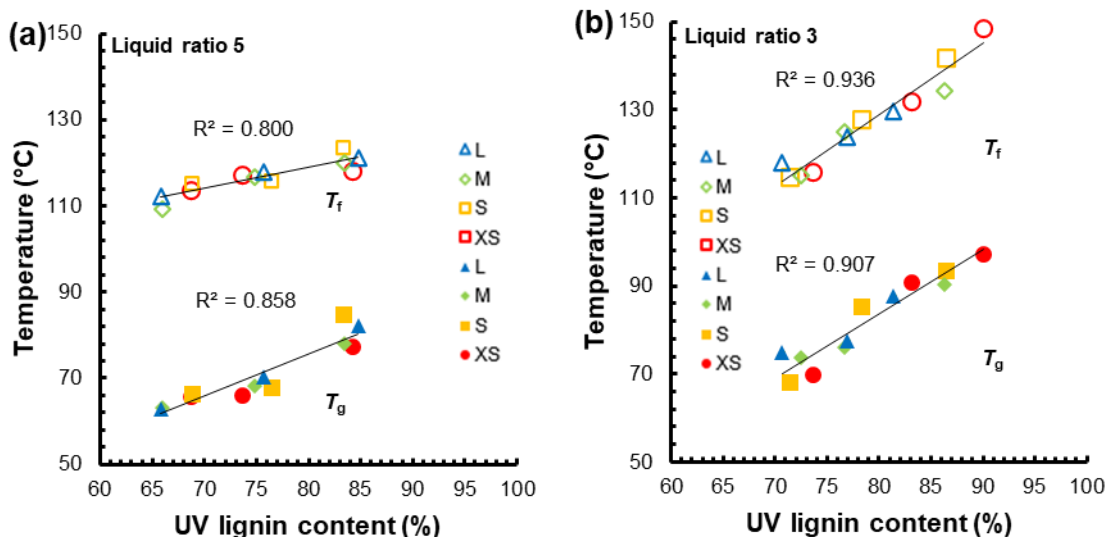
Fig. 6. Relationship between the thermal flow behavior and UV lignin content of GL400 samples: (a) liquid ratio 5, (b) liquid ratio 3

CONCLUSIONS

1. Acid-catalyzed poly(ethylene glycol) (PEG400) solvolysis of cedar wood meal was conducted using four classified wood meal sizes and two liquid ratios of 3 and 5. A similar level of glycolyzed lignin (GL400) yields was obtained at both liquid ratios. However, the properties of GL400 varied significantly depending on the reaction conditions.

2. The PEG liquid ratio strongly influenced the physical properties of the GL400 samples. For example, maximum differences of ~20 °C for T_g and ~30 °C for T_f were determined between the liquid ratios 5 and 3 for extra small (XS)-sized wood meal at the 240-min reaction time.

3. A positive correlation was observed between the UV lignin content and T_g and T_f of GL400 samples at both liquid ratios.

ACKNOWLEDGMENTS

REFERENCES CITED

Achyuthan, K. E., Achyuthan, A. M., Adams, P. D., Dirk, S. M., Harper, J. C. Simmons, B. A., and Singh, A. K. (2010). "Supramolecular self-assembled chaos: Polyphenolic lignin's barrier to cost-effective lignocellulosic biofuels," *Molecules* 15, 8641-8688.

Ai, X., Feng, S., Shui, T., Kakkar, H., and Xu, C. C. (2021). "Effects of alcell lignin methylolation and lignin adding stage on lignin-based phenolic adhesives," *Molecules* 26(22), article 6762. DOI: 10.3390/molecules26226762

Anttila, J., Tanskanen, J., Rousu, P., Rousu, P., and Hytönen, K. (2010). "Process for preparing a sugar product," U.S. Patent No. US20100240112A1.

Argyropoulos, D. D. S., Crestini, C., Dahlstrand, C., Furusjö, E., Gioia, C., Jedvert, K., Henriksson, G., Hulteberg, C., Lawoko, M., Pierrou, C., Samec, J. S. M., Subbotina, E., Wallmo, H., and Wimby, M. (2023). "Kraft lignin: A valuable, sustainable resource, opportunities and challenges," *ChemSusChem* 16(23), article e202300492. DOI: 10.1002/cssc.202300492

Beaucamp, A., Culebras, M., and Collins, M. N. (2021). "Sustainable mesoporous carbon nanostructures derived from lignin for early detection of glucose," *Green Chemistry* 23(15). DOI: 10.1039/D1GC02062E

Covinich, L. G., and Area, M. C. (2024). "Trends and limitations of lignin as a starting material," *BioResources* 19(1), 6-9. DOI: 10.15376/biores.19.1.6-9

Demuner, I. F., Colodette, J. L., Demuner, A. J., and Jardim, C. M. (2019). "Biorefinery review: Wide-reaching products through kraft lignin," *BioResources* 14(3), 7543-7581. DOI: 10.15376/biores.14.3.Demuner

Dence, C. W., and Lin, S. Y. (1992). "Introduction," in: *Methods in Lignin Chemistry; Springer Series in Wood Science*, C. W. Dence, and S. Y. Lin (eds.), Springer, Berlin, Germany, pp. 1-19.

Kobayashi, A., Kobayashi, F., Ebina, T., Ishii, R., Nakamura, T., Nge, T. T., Yamada, T., Shiraishi, A., and Yamashita, T. (2018). "Effect of thermal base generators on the FRP fabrication with glycol-lignin," *J. Photopol. Sci. Technol.* 31(1), 101-106. DOI: 10.2494/photopolymer.31.101

Kopsahelis, N., Agouridis, N., Bekatorou, A., and Kanellaki, M. (2007). "Comparative study of spent grains and delignified spent grains as yeast supports for alcohol production from molasses," *Bioresource Technology* 98, 1440-1447.

Kupiainen, L., Ahola, J., and Tanskanen, J. (2012). "Hydrolysis of organosolv wheat pulp in formic acid at high temperature for glucose production," *Bioresource Technology* 116, 29-35. DOI: 10.1016/j.biortech.2012.04.012

Matsushita, Y. (2015). "Conversion of technical lignins to functional materials with retained polymeric properties," *Journal of Wood Science* 61(3), article 230. DOI: 10.1007/s10086-015-1470-2

Nge, T. T., Takata, E., Takahashi, S., and Yamada, T. (2016). "Isolation and thermal characterization of softwood-derived lignin with thermal flow properties," *ACS Sustain. Chem. Eng.* 4(5), 2861-2868. DOI: 10.1021/acssuschemeng.6b00447

Nge, T. T., Tobimatsu, Y., Takahashi, S., Takata, E., Yamamura, M., Miyagawa, Y., Ikeda, T., Umezawa, T., and Yamada, T. (2018). "Isolation and characterization of polyethylene glycol (PEG)-modified glycol lignin via PEG solvolysis of softwood biomass in a large-scale batch reactor," *ACS Sustain. Chem. Eng.* 6(6), 7841-7848. DOI: 10.1021/acssuschemeng.8b00965

Nge, T. T., Tobimatsu, Y., Yamamura, M., Takahashi, S., Takata, E., Umezawa, T., and Yamada, T. (2020). "Effect of heat treatment on the chemical structure and thermal properties of softwood-derived glycol lignin," *Molecules* 25, article 1167. DOI: 10.3390/molecules25051167

Ono, K., Tanaike, O., Ishii, R., Nakamura, T., Shikinaka, K., Ebina, T., Nge, T. T., and Yamada, T. (2019). "Solvent-free fabrication of an elastomeric epoxy resin using glycol lignin from Japanese cedar," *ACS Omega* 4(17), 17251-17256. DOI: 10.1021/acsomega.9b01884

Osti, N. C., Remy, R. A., Mamontov, E., Advincula, R., and Nguyen, N. A. (2024). "Designing a dynamic material via interlocking kraft lignin with ultrahigh molecular weight poly(ethylene oxide)," *ACS Applied Polymer Materials* 6(19), 11877-11888. DOI: 10.1021/acsapm.4c01971

Pye, E. K., and Lora, J. H., (1991) "The Alcell process: A proven alternative to kraft pulping," *TAPPI Journal* 74, 113-118.

Rabelo, S. C., Nakasu, P. Y. S., Scopel, E., Araújo, M. F., Cardoso, L. H., and Costa, A. C. da. (2023). "Organosolv pretreatment for biorefineries: Current status, perspectives, and challenges," *Bioresource Technology* 369, article 128331. DOI: 10.1016/j.biortech.2022.128331

Rodrigues, J. S., de Freitas, A. de S. M., Maciel, C. C., Mendes, S. F., Diment, D., Balakshin, M., and Botaro, V. R. (2023). "Selection of kraft lignin fractions as a partial substitute for phenol in synthesis of phenolic resins: Structure-property correlation," *Industrial Crops and Products* 191, article 115948. DOI: 10.1016/j.indcrop.2022.115948

Shorey, R., and Mekonnen, T. H. (2024). "Oleic acid decorated kraft lignin as a hydrophobic and functional filler of cellulose acetate films," *International Journal of Biological Macromolecules* 268, article 131672. DOI: 10.1016/j.ijbiomac.2024.131672

Suzuki, A., Ishii, R., Yoshida, H., Ebina, T., Nge, T. T., and Yamada, T. (2018). "Microstructure and properties of clay glycol lignin nanocomposite films using different mixed solvents," *Clay Science* 22, 71-78. DOI: 10.11362/jcssjclayscience.22.3_71

Suzuki, A., Shikinaka, K., Ishii, R., Yoshida, H., Ebina, T., Ishida, T., Nge, T. T., and Yamada, T. (2019). "Heat-resistant insulation film containing clay and wood components," *Appl. Clay Sci.* 180, article ID 105189. DOI: 10.1016/j.clay.2019.105189

Takahashi, K., Ishii, R., Nakamura, T., Suzuki, A., Ebina, T., Yoshida, M., Kubota, M., Nge, T. T., and Yamada, T. (2017). "Flexible electronic substrate film fabricated using natural clay and wood components with cross-linking polymer," *Adv. Mater.* 29(17), article ID 1606512. DOI: 10.1002/adma.201606512

Takata, E., Nge, T. T., Takahashi, S., Ohashi, Y., and Yamada, T. (2016). "Acidic solvolysis of softwood in recycled polyethylene glycol system," *BioResources* 11(2), 4446-4458.

Tofani, G., Jasiukaitytė-Grojzdek, E., Grilc, M., and Likozar, B. (2023). "Organosolv biorefinery: resource-based process optimisation, pilot technology scale-up and economics," *Green Chemistry* 26(1), and 186. DOI: 10.1039/d3gc03274d

Van Nieuwenhove, I., Renders, T., Lauwaert, J., De Roo, T., De Clercq, J., and Verberckmoes, A. (2020). "Biobased resins using lignin and glyoxal," *ACS*

Sustainable Chemistry & Engineering 51, article 18789. DOI: 10.1021/acssuschemeng.0c07227

Wang, C., Kelley, S. S., and Venditti, R. A. (2016). "Lignin-based thermoplastic materials," *ChemSusChem* 9(8), 770-783. DOI: 10.1002/cssc.201501531

Yamada, T., Takata, E., Takahashi, S., Nge, T. T., and Ikeda, T. (2021). "Glycol lignin production method and its system," JP. Patent No. 6890821B2.